Inorganica Chimica Acta, *192* (1992) 173–181

X-ray structural studies of $FeBr_2 \cdot 4H_2O$, $CoBr_2 \cdot 4H_2O$, $NiCl_2 \cdot 4H_2O$ and $CuBr_2 \cdot 4H_2O$. *cis/trans* Selectivity in transition metal(II) dihalide tetrahydrate

Kenji Waizumi*
Institute of Mineralogy, Petrology and Economic Geology, Faculty of Science, Tohoku University, Aoba, Sendai 980 (Japan)

Hideki Masuda** and Hitoshi Ohtaki†
Coordination Chemistry Laboratories, Institute for Molecular Science, Myodaiji, Okazaki 444 (Japan)

(Received October 9, 1991)

Abstract

Crystal structures of $FeBr_2 \cdot 4H_2O$ (**1**), $CoBr_2 \cdot 4H_2O$ (**2**), $NiCl_2 \cdot 4H_2O$ (**3**) and $CuBr_2 \cdot 4H_2O$ (**4**) have been determined by the X-ray diffraction method. **1** crystallizes in the monoclinic form with the space group $P2_1/a$ having the unit cell dimensions of $a=8.730(2)\times10^2$, $b=7.239(1)\times10^2$, $c=6.149(2)\times10^2$ pm, $\beta=110.72(2)°$, $V=363.5\times10^6$ pm^3 and $Z=2$; **2** monoclinic, $P2_1/a$, $a=8.581(5)\times10^2$, $b=7.143(4)\times10^2$, $c=6.180(2)\times10^2$ pm, $\beta=110.29(4)°$, $V=355.3\times10^6$ pm^3 and $Z=2$; **3** monoclinic, $P2_1/a$, $a=13.378(3)\times10^2$, $b=9.301(3)\times10^2$, $c=5.988(1)\times10^2$ pm, $\beta=126.45(1)°$, $V=599.4\times10^6$ pm^3 and $Z=4$; **4** monoclinic, $P2_1/a$, $a=12.013(3)\times10^2$, $b=7.330(4)\times10^2$, $c=4.116(2)\times10^2$ pm, $\beta=105.44(3)°$, $V=349.3\times10^6$ pm^3 and $Z=2$. The hexa-coordinated geometry around the Fe^{2+} and Co^{2+} ions in **1** and **2**, respectively, is a distorted *trans*-octahedron with four aqua oxygens at the equatorial position and two Br^- ions at the axial position, whereas the hexa-coordinated central Ni^{2+} ion in **3** has a distorted *cis*-octahedral geometry with three aqua oxygens and one Cl^- ion at the equatorial position and one aqua oxygen and one Cl^- ion at the axial position. The central Cu^{2+} ion in **4** has an axially elongated octahedral form with two Br^- ions and two aqua oxygens at the equatorial position, and two Br^- ions belonging to the adjacent units locate at the axial position of the copper(II) ion. The remaining two water molecules in the compound are situated outside the coordination sphere of the copper(II) ion and are connected to the water molecule in the coordination sphere of a copper(II) ion with a Br^- ion in an adjacent copper(II) complex by hydrogen bonds. The *cis/trans* selectivity in the transition metal(II) dihalide tetrahydrate complexes is discussed in terms of the electronic configuration of the central metal(II) ions, the repulsive interaction between halide ions due to the steric effect, and the effect of hydrogen bonds.

Introduction

Transition metal(II) dihalides form various hydration states such as di-, tetra- and hexahydrates in the solid state. Among them, the metal ions in dihydrate crystals such as $MnCl_2 \cdot 2H_2O$ [1], $MnBr_2 \cdot 2H_2O$ [2], $FeCl_2 \cdot 2H_2O$ [1], $CoCl_2 \cdot 2H_2O$ [3], $CoBr_2 \cdot 2H_2O$ [2] and $NiCl_2 \cdot 2H_2O$ [4] are octahedrally coordinated with four halogen ions in the square plane and two water molecules at the axial position to form the $[MX_4(H_2O)_2]$ unit. The Cu^{2+} ion in the $CuCl_2 \cdot 2H_2O$ crystal forms an elongated octahedron with two Cu–O and two Cu–Cl bonds in the square plane and two long Cu–Cl bonds along the axis perpendicular to the plane [5]. The difference between the configurations of $CuCl_2 \cdot 2H_2O$ and those of the other dihydrates has been interpreted in terms of the Jahn–Teller effect [6]. The metal ions in hexahydrate crystals reported hitherto for $CoCl_2 \cdot 6H_2O$ [7], $CoBr_2 \cdot 6H_2O$ [8], $NiCl_2 \cdot 6H_2O$ [9] and $NiBr_2 \cdot 6H_2O$ [10] are all octahedrally coordinated with four water molecules at the equatorial position and two halide ions at the axial position, in which each halide ion is linked to the remaining water molecule outside the coordination shell of the metal ions by hydrogen bonds.

On the other hand, the crystal structure of the tetrahydrate complexes is known to be of two kinds. One is the *trans*-configuration structure with respect

---

*Present address: Coordination Chemistry Laboratories, Institute for Molecular Science, Myodaiji, Okazaki 444, Japan.

**Present address: Department of Chemistry, Faculty of Science, Nagoya University, Chikusa-ku, Nagoya 464-01, Japan.

†Author to whom correspondence should be addressed.

0020-1693/92/$5.00

to the halide ions; examples are $CrCl_2 \cdot 4H_2O$ [11] and $FeCl_2 \cdot 4H_2O$ [12]. The other is the *cis* structure in which three water molecules and one halide ion at the equatorial position and one water molecule and one halide ion at the axial position form a distorted octahedron around the metal ion. $MnCl_2 \cdot 4H_2O$ [13], $MnBr_2 \cdot 4H_2O$ [14] and $CoCl_2 \cdot 4H_2O$ [7b] belong to this category. Therefore, it is interesting to consider factors controlling *cis*/*trans* configurations in the transition metal(II) dihalide tetrahydrate complexes.

The structure of $NiCl_2 \cdot 4H_2O$ was originally reported to consist of $[Ni(H_2O)_6]^{2+}$ and $[NiCl_6]^{4-}$ in the ratio 2:1 [15], but later it was suggested that it was isostructural with the $MnCl_2 \cdot 4H_2O$ crystal [16]. Since this problem has remained unsolved, we decided to study the structure of $NiCl_2 \cdot 4H_2O$.

In this paper we present the crystal data of $FeBr_2 \cdot 4H_2O$, $CoBr_2 \cdot 4H_2O$, $NiCl_2 \cdot 4H_2O$ and $CuBr_2 \cdot 4H_2O$ and discuss the stereoselectivity of the *cis*/*trans* configurations of the complexes.

Experimental

Preparation

Greenish transparent crystals of $FeBr_2 \cdot 4H_2O$ (**1**) suitable for X-ray examination were precipitated in the form of approximately rhombic thin plates from an $FeBr_2$ aqueous solution at 65 °C according to the solubility curve [17]. $CoBr_2 \cdot 4H_2O$ (**2**) was obtained as dark red cubo-octahedral crystals from a $CoBr_2$ aqueous solution at 50 °C [18], and $NiCl_2 \cdot 4H_2O$ (**3**) was obtained as light greenish cubo-octahedral crystals from an $NiCl_2$ aqueous solution at 50 °C [19]. $CuBr_2 \cdot 4H_2O$ (**4**) was crystallized as dark green needle-like crystals from a $CuBr_2$ aqueous solution at 0 °C [20].

X-ray structural determinations

Experimental details and crystal data for the four structures are listed in Table 1. Diffraction data were collected with Enraf-Nonius CAD4 and Rigaku AFC-5R four-circle diffractometers using graphite mono-

TABLE 1. Crystal data and experimental conditions

	1	**2**	**3**	**4**
Formula	$FeBr_2 \cdot 4H_2O$	$CoBr_2 \cdot 4H_2O$	$NiCl_2 \cdot 4H_2O$	$CuBr_2 \cdot 4H_2O$
M_r	287.73	290.81	201.68	295.42
Crystal system	monoclinic	monoclinic	monoclinic	monoclinic
Space group	$P2_1/a$	$P2_1/a$	$P2_1/a$	$P2_1/a$
a ($\times 10^2$ pm)	8.730(2)	8.581(5)	13.378(3)	12.013(3)
b ($\times 10^2$ pm)	7.239(1)	7.143(4)	9.301(3)	7.330(4)
c ($\times 10^2$ pm)	6.149(2)	6.180(2)	5.988(1)	4.116(2)
β (°)	110.72(2)	110.29(4)	126.45(1)	105.44(3)
V ($\times 10^6$ pm^3)	363.5	355.3	599.4	349.3
T (°C)	297	297	297	240
$F(000)$	272	274	408	278
Radiation (Mo Kα) ($\times 10^2$ pm)	0.71073	0.71073	0.71073	0.71073
D_c (g/cm^3)	2.629	2.718	2.235	2.808
Z	2	2	4	2
Crystal size (mm)	$0.2 \times 0.4 \times 0.4$	$0.4 \times 0.4 \times 0.4$	$0.3 \times 0.4 \times 0.4$	$0.1 \times 0.1 \times 0.2$
μ(Mo Kα) (cm^{-1})	137.1	143.6	40.7	156.7
Diffractometer	CAD4	AFC5R	AFC5R	CAD4
Unit cell determination	25 reflections, $19.60 \leqslant 2\theta \leqslant 30.47°$	20 reflections, $18.24 \leqslant 2\theta \leqslant 21.20°$	20 reflections, $18.24 \leqslant 2\theta \leqslant 21.15°$	25 reflections, $15.16 \leqslant 2\theta \leqslant 31.04°$
Scan mode	ω–2θ	ω–2θ	ω–2θ	ω–2θ
Maximum 2θ (°)	60	60	60	60
hkl range	± 8, $+10$, $+12$	$+12$, $+10$, ± 8	$+18$, $+13$, ± 8	± 5, $+10$, $+16$
Scanning rate (°/min)	4	4	4	4
Scan width (°)	$1.0 + 0.35 \tan \theta$	$0.8 + 0.5 \tan \theta$	$1.2 + 0.5 \tan \theta$	$0.8 + 0.35 \tan \theta$
Cutoff type	$\lvert I_o \rvert > 3\sigma \lvert I_o \rvert$	$\lvert F_o \rvert > 3\sigma \lvert F_o \rvert$	$\lvert F_o \rvert > 3\sigma \lvert F_o \rvert$	$\lvert I_o \rvert > 3\sigma \lvert I_o \rvert$
Reflections measured	1201	1091	2033	1140
Reflections after cutoff	776	843	1507	317
Parameters refined	51	51	94	51
R	0.039	0.050	0.055	0.066
R_w	0.045	0.062	0.067	0.074
Weighting schemes	$\{[\sigma(\lvert F_o \rvert)]^2 + (0.020\lvert F_o \rvert)^2\}^{-1}$	$\{[\sigma(\lvert F_o \rvert)]^2 + (0.035\lvert F_o \rvert)^2\}^{-1}$	$\{[\sigma(\lvert F_o \rvert)]^2 + (0.015\lvert F_o \rvert)^2\}^{-1}$	$\{[\sigma(\lvert F_o \rvert)]^2 + (0.020\lvert F_o \rvert)^2\}^{-1}$

chromated Mo Kα radiation for **1**, **4** and **2**, **3**, respectively. The intensities were monitored by three standard reflections every 2 h for **1** and **4**, or every 100 reflections for **2** and **3**. There was no significant variation in intensities during the data collections. The intensities were converted to F_0 data in the usual manner. All the reflections were corrected for Lorentz and polarization effects. An empirical absorption correction using DIFABS [21] was applied after isotropic refinement for **1**, **2**, **3** and **4** with corrections in the range 0.99–1.03, 0.98–1.00, 0.99–1.01 and 0.92–1.00, respectively.

The four crystal structures were determined by the heavy atom method and refined by the full matrix least-squares method. Several cycles of refinement including

TABLE 2. Positional coordinates ($\times 10^4$; for H$\times 10^3$), equivalent isotropic temperature factors for non-H atoms and isotropic temperature factors for H atoms[a]

	x	y	z	B_{eq} or B_{iso} ($\times 10^4$ pm^2)
Complex **1**				
Fe	0	0	0	1.8
Br	794.6(8)	−2662.6(9)	3208(1)	2.3
O(1)	2423(5)	10(7)	17(9)	3.2
O(2)	−642(6)	−2047(7)	−2531(7)	2.7
H(1A)	277(10)	58(13)	−123(12)	7.8
H(1B)	325(10)	−43(14)	133(14)	8.7
H(2A)	−145(7)	−163(8)	−375(9)	5.3
H(2B)	17(9)	−211(11)	−321(11)	5.2
Complex **2**				
Co	0	0	0	1.3
Br	788(1)	−2607(1)	3177(1)	1.8
O(1)	2417(5)	14(6)	29(9)	2.9
O(2)	−603(6)	−2079(6)	−2465(7)	2.4
H(1A)	263(13)	38(14)	−89(17)	4.4
H(1B)	328(11)	−63(13)	123(14)	2.8
H(2A)	−184(11)	−149(13)	−367(15)	3.8
H(2B)	17(16)	−142(21)	−370(22)	9.1
Complex **3**				
Ni	7638.8(4)	1689.2(5)	7774.9(9)	1.0
Cl(1)	6206.6(8)	3630(1)	5918(2)	1.5
Cl(2)	9291.3(9)	3058(1)	8330(2)	1.6
O(1)	8372(3)	2252(3)	11832(5)	1.5
O(2)	6954(3)	1159(3)	3724(5)	1.5
O(3)	8689(3)	−159(4)	9076(6)	2.1
O(4)	6319(3)	414(4)	7571(7)	2.1
H(1A)	908(5)	217(7)	1272(12)	2.8
H(1B)	802(5)	185(6)	1250(11)	2.1
H(2A)	616(6)	155(8)	228(14)	3.8
H(2B)	695(5)	−39(7)	377(11)	3.2
H(3A)	815(8)	−60(11)	787(17)	8.4
H(3B)	931(7)	−28(9)	880(16)	7.3
H(4A)	581(6)	73(7)	748(13)	3.6
H(4B)	652(5)	−51(6)	804(12)	2.8
Complex **4**				
Cu	0	0	0	1.6
Br	213(3)	−2442(3)	4099(5)	2.0
O(1)	1628(16)	553(19)	1484(29)	2.0
O(2)	2978(18)	−507(22)	−2485(33)	2.7
H(1A)	196(21)	38(3)	26(39)	2.1
H(1B)	195(25)	3(47)	355(45)	5.8
H(2A)	359(28)	2(48)	−273(49)	7.4
H(2B)	322(29)	−152(38)	−226(57)	6.5

[a] Anisotropically refined non-H atoms are given in the form of the equivalent displacement parameter defined as: $B_{eq}=4/3[a^2\beta_{11}+ab(\cos\gamma)\beta_{12}\cdots]$ for **1** and **4**, and $B_{eq}=4/3[a^2\beta_{11}+2ab(\cos\gamma)\beta_{12}\cdots]$ for **2** and **3**.

that for anisotropic thermal parameters for non-hydrogen atoms were carried out. Location of all H atoms was determined by the Fourier difference synthesis and was refined isotropically. Atomic scattering factors and anomalous dispersion terms were taken from the International Tables for X-ray Crystallography [22, 23]. Calculations for **1** and **4** were performed on a Micro VAX II computer using the Enraf-Nonius SDP program [24], and those for **2** and **3** were performed on a HITAC M-680H computer at the Computer Center of the Institute for Molecular Science by using the program system UNICS III [25]. The final atomic parameters for **1**, **2**, **3** and **4** are summarized in Table 2.

Results and discussion

The coordination structures of transition metals in **1**, **2**, **3** and **4** are shown in Fig. 1 with the atomic numbering by ORTEP [26] drawing. The bond lengths and bond angles are listed in Table 3. The crystal structures of the compounds are also shown in Figs. 2–5 with hydrogen bonds represented by broken lines.

The crystal of **1** is isostructural with $FeCl_2 \cdot 4H_2O$ [13]. The structure around the Fe^{2+} ion is slightly distorted octahedral with the *trans* configuration with respect to the Br^- ions. In the crystal the octahedral units are connected with each other by hydrogen bonds (broken lines in Fig. 2); $Br_{IV} \cdots O_I(1) = 3.373(6) \times 10^2$ pm, $Br' \cdots O_I(1) = 3.364(4) \times 10^2$ pm, $Br_{III} \cdots O'_I(2) = 3.289(4) \times 10^2$ pm and $Br_{II} \cdots O(2) = 3.310(5) \times 10^2$ pm.

The structure around the Co^{2+} ion of **2** is also the *trans* configuration with respect to the Br^- ions as in $FeCl_2 \cdot 4H_2O$ [13] and $FeBr_2 \cdot 4H_2O$. This is different from $CoCl_2 \cdot 4H_2O$ which has the *cis* configuration [7b]. The lengths of the hydrogen bonds in Fig. 3 are $Br' \cdots O_I(1) = 3.348(4) \times 10^2$ pm, $Br_{IV} \cdots O_I(1) = 3.362(6) \times 10^2$ pm, $Br_{II} \cdots O(2) = 3.324(6) \times 10^2$ pm and $Br_{III} \cdots O'_I(2) = 3.333(5) \times 10^2$ pm.

The structure around the Ni^{2+} ion of **3** is distorted octahedral with the *cis* configuration with respect to the Cl^- ions. The molecular structure is isostructural with those of $CoCl_2 \cdot 4H_2O$ [7b], $MnCl_2 \cdot 4H_2O$ [13] and $MnBr_2 \cdot 4H_2O$ [14] as suggested by McElearney *et al.*

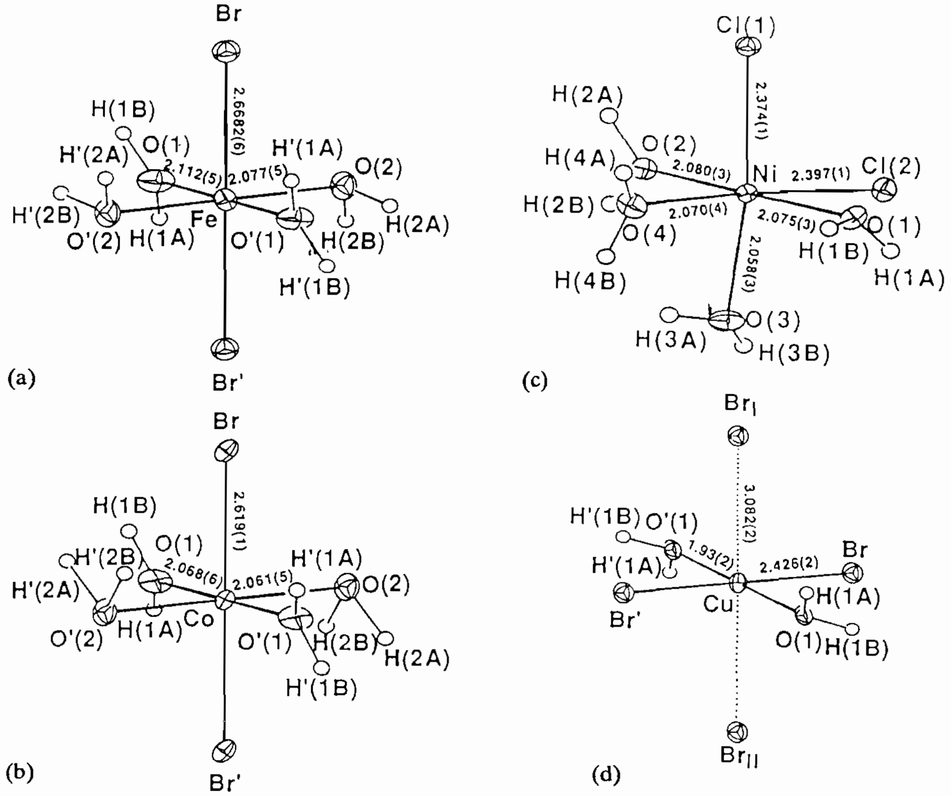

Fig. 1. ORTEP drawings [26] of the molecular structure of (a) $FeBr_2 \cdot 4H_2O$, (b) $CoBr_2 \cdot 4H_2O$, (c) $NiCl_2 \cdot 4H_2O$ and (d) $CuBr_2 \cdot 4H_2O$ with thermal ellipsoids scaled at 30% probability level. The bond lengths are in $pm \times 10^2$. H atoms are represented by circles of 0.1×10^2 pm.

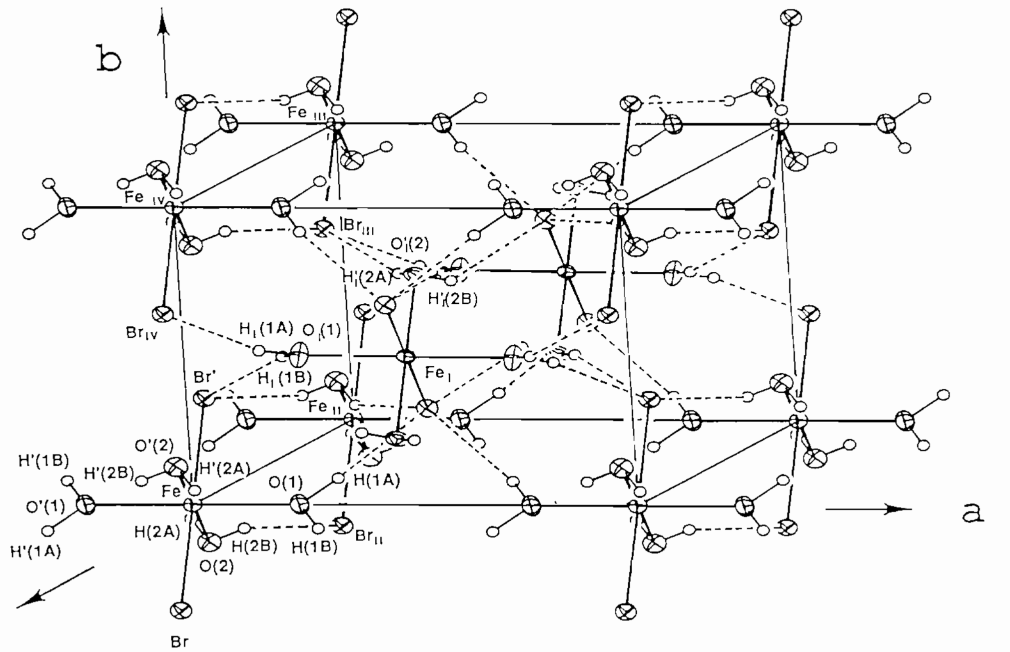

Fig. 2. An ORTEP drawing [26] of the crystal structure in $FeBr_2\cdot 4H_2O$ unit cell with thermal ellipsoids scaled at 30% probability level. H atoms are represented by circles of 0.1×10^2 pm.

TABLE 3. Selected interatomic distances ($\times 10^2$ pm) and angles (°)[a]

Complex **1**			
Fe–Br	2.6682(6)	Fe–O(1)	2.112(5)
Fe–O(2)	2.077(5)		
Br–Fe–Br'	180	Br–Fe–O(1)	90.1(1)
Br–Fe–O'(1)	89.9(1)	Br–Fe–O(2)	88.2(1)
Br–Fe–O'(2)	91.8(1)	Br'–Fe–O(1)	89.9(2)
Br'–Fe–O'(1)	90.1(1)	Br'–Fe–O(2)	91.8(1)
Br'–Fe–O'(2)	88.2(1)		
O(1)–Fe–O(2)	90.6(2)	O(1)–Fe–O'(1)	180
O(1)–Fe–O'(2)	89.4(2)	O'(1)–Fe–O(2)	89.4(2)
O'(1)–Fe–O'(2)	90.9(2)	O(2)–Fe–O'(2)	180
Complex **2**			
Co–Br	2.619(1)	Co–O(1)	2.068(6)
Co–O(2)	2.061(5)		
Br–Co–Br'	180	Br–Co–O(1)	90.0(2)
Br–Co–O'(1)	90.0(2)	Br–Co–O(2)	88.6(2)
Br–Co–O'(2)	91.4(2)	Br'–Co–O(1)	90.0(2)
Br'–Co–O'(1)	90.0(2)	Br'–Co–O(2)	88.6(2)
Br'–Co–O'(2)	91.4(2)		
O(1)–Co–O(2)	90.2(2)	O(1)–Co–O'(1)	180
O(1)–Co–O'(2)	89.8(2)	O'(1)–Co–O(2)	89.8(2)
O'(1)–Co–O'(2)	90.2(2)	O(2)–Co–O'(2)	180
Complex **3**			
Ni–Cl(1)	2.374(1)	Ni–Cl(2)	2.397(1)
Ni–O(1)	2.075(3)	Ni–O(2)	2.080(3)
Ni–O(3)	2.058(3)	Ni–O(4)	2.070(4)
Cl(1)–Ni–Cl(2)	94.72(5)	Cl(1)–Ni–O(1)	92.59(9)
Cl(1)–Ni–O(2)	87.7(1)	Cl(1)–Ni–O(3)	172.77(9)
Cl(1)–Ni–O(4)	89.2(1)	Cl(2)–Ni–O(1)	87.0(1)
Cl(2)–Ni–O(2)	91.1(1)	Cl(2)–Ni–O(3)	91.5(1)
Cl(2)–Ni–O(4)	175.4(8)	O(1)–Ni–O(2)	178.1(2)
O(1)–Ni–O(3)	91.5(1)	O(1)–Ni–O(4)	90.4(2)
O(2)–Ni–O(3)	88.4(1)	O(2)–Ni–O(4)	91.5(2)
O(3)–Ni–O(4)	84.8(2)		
Complex **4**[b]			
Cu–Br	2.426(2)	Cu–Br_I	3.082(2)
Cu–O(1)	1.93(2)		
Br–Cu–Br'	180	Br–Cu–Br_I	95.97(7)
Br–Cu–Br_{II}	84.03(7)	Br–Cu–O(1)	91.4(4)
Br–Cu–O'(1)	88.6(4)	Br'–Cu–Br_I	84.03(7)
Br'–Cu–Br_{II}	95.97(7)	Br'–Cu–O(1)	88.6(4)
Br'–Cu–O'(1)	91.4(4)		
Br_I–Cu–Br_{II}	180	Br_I–Cu–O(1)	94.7(4)
Br_I–Cu–O'(1)	85.3(4)	Br_{II}–Cu–O(1)	85.3(4)
Br_{II}–Cu–O'(1)	94.7(4)	O(1)–Cu–O'(1)	180

[a] The primed and unprimed atoms are related by a center of symmetry to each other. [b] Br_I and Br_{II} are the symmetry equivalent of Br at $x, y, -1+z$ and $-x, -y, 1-z$, respectively.

[16]. The Ni–O(3) bond length in this complex is shorter than the lengths of the Ni–O(1), Ni–O(2), Ni–O(3) bonds and the length of the Ni–Cl(1) bond is shorter than that of the Ni–Cl(2) bond. Thus the complex is considered to be axially compressed; similar structures are also found in the *cis*-octahedral $MnCl_2\cdot 4H_2O$ [13], $MnBr_2\cdot 4H_2O$ [14] and $CoCl_2\cdot 4H_2O$ complexes [7b]. The Ni^{2+} ion is displaced by $0.048(2)\times 10^2$ pm out of the plane defined by the three water oxygen andone Cl^- ion towards the axial chloride ion. The network of hydrogen bonds is formed among

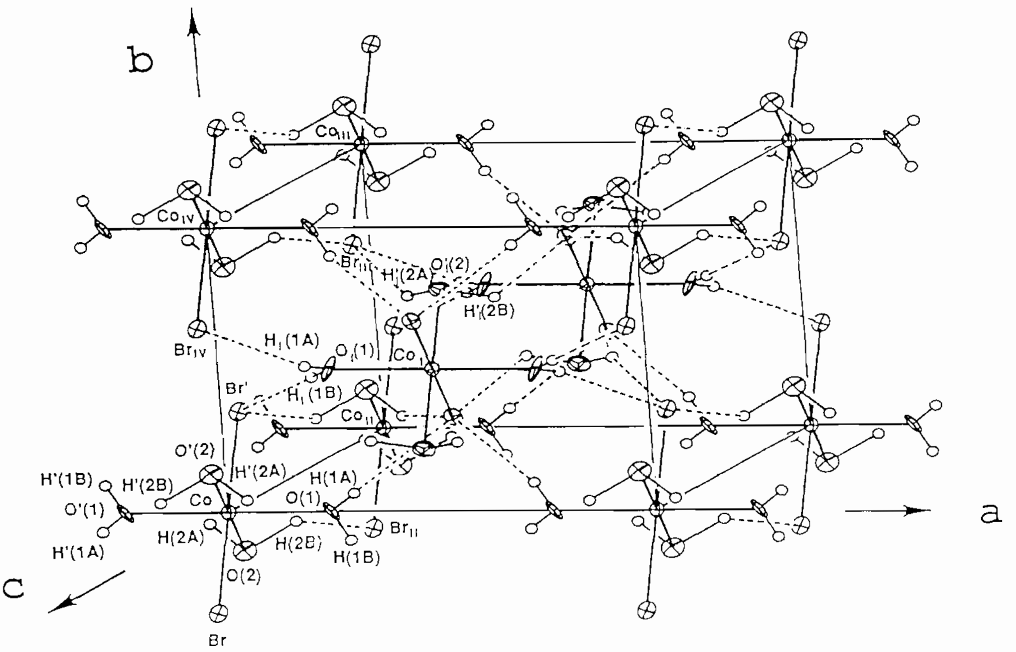

Fig. 3. An ORTEP drawing [26] of the crystal structure in $CoBr_2 \cdot 4H_2O$ unit cell with thermal ellipsoids scaled at the 30% probability level. H atoms are represented by circles with 0.1×10^2 pm.

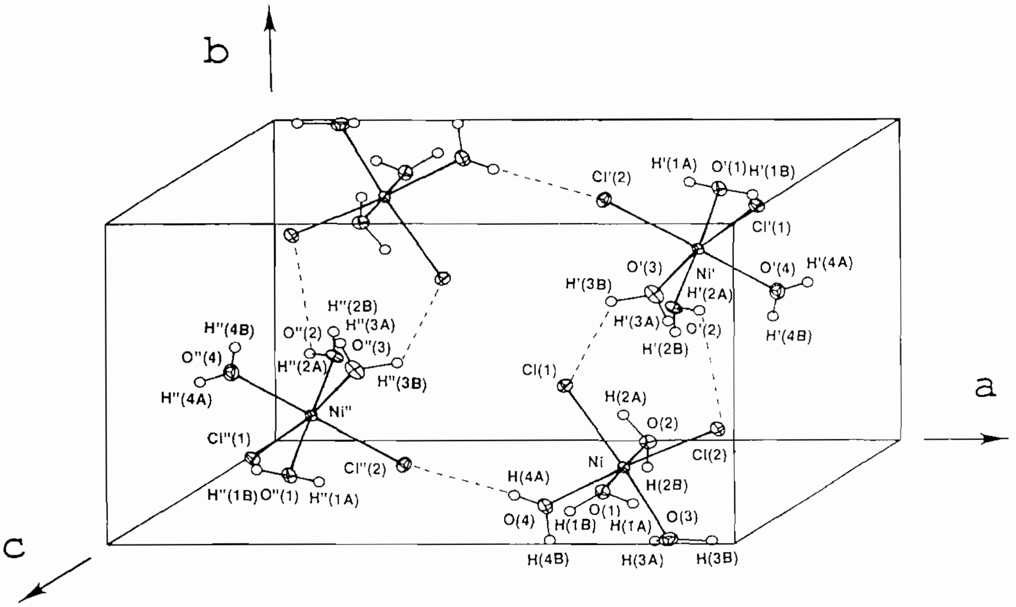

Fig. 4. An ORTEP drawing [26] of the crystal structure in $NiCl_2 \cdot 4H_2O$ with thermal ellipsoids scaled at the 30% probability level. H atoms are represented by circles with 0.1×10^2 pm.

discrete octahedral units with the distances of $Cl(1) \cdots O'(3) = 3.275(2) \times 10^2$, $Cl(2) \cdots O'(2) = 3.159(2) \times 10^2$, and $Cl''(2) \cdots O(4) = 3.324(2) \times 10^2$ pm.

The structure of **4** is different from those of the other transition metal dihalide tetrahydrate complexes. The structure around the Cu^{2+} ion is axially elongated octahedral with two Br^- ions and two aqua oxygens at the equatorial position and two Br^- ions belonging to the adjacent units at the axial position. The remaining two water molecules are located out of the first coordination sphere and connected to the coordinated water and bromide ion by hydrogen bonds. In the crystal the discrete $[CuBr_2(H_2O)_2]$ units are connected with the uncoordinated water molecules by hydrogen bonds (Fig. 5); $Br_{III} \cdots O_{IV}(2) = 3.31(2) \times 10^2$ pm, $O(1) \cdots O_{IV}(2) = 2.94(2) \times 10^2$ pm, $O'(1) \cdots O'(2) =$

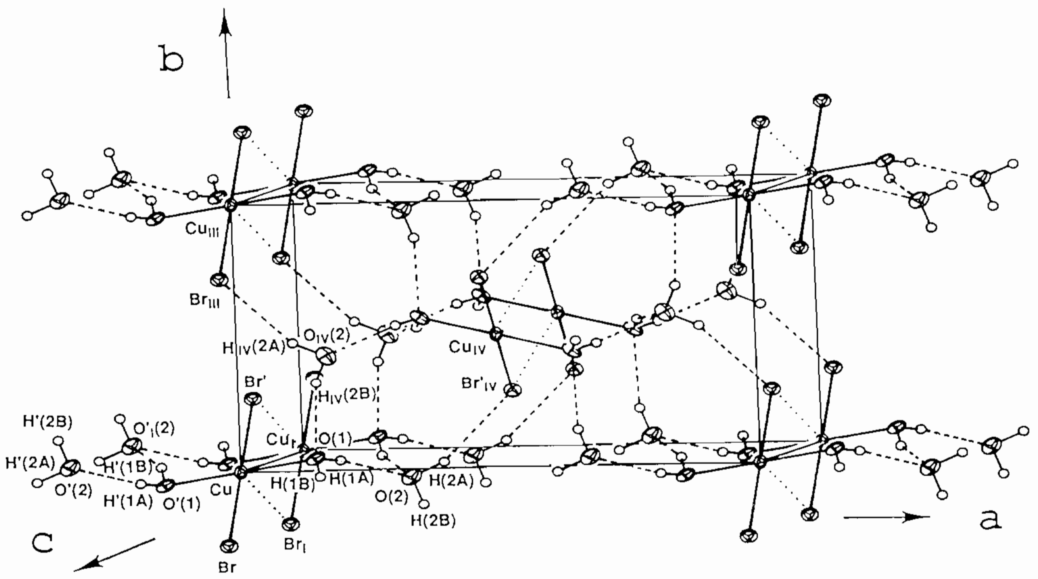

Fig. 5. An ORTEP drawing [26] of the crystal structure in $CuBr_2 \cdot 4H_2O$ unit cell with thermal ellipsoids scaled at the 30% probability level. H atoms are represented by circles with 0.1×10^2 pm.

TABLE 4. Distances between transition metal and ligands and the sum of the ionic radii ($\times 10^2$ pm)[a]

	Cr^{2+} [0.80]	Mn^{2+} [0.83]	Fe^{2+} [0.78]	Co^{2+} [0.745]	Ni^{2+} [0.69]	Cu^{2+} [0.73]
Chloride complexes						
Type	*trans*	*cis*	*trans*	*cis*	*cis*	[g]
Cl^-	2.758[b]	2.475[c]	2.526[d]	2.406[e]	2.374[f]	
[1.81]		2.500[c]		2.422[e]	2.397[f]	
	(2.61)	(2.63)	(2.59)	(2.555)	(2.50)	
$O(H_2)$	2.081[b]	2.224[c]	2.117[d]	2.115[e]	2.075[f]	
[1.40]	2.074[b]	2.185[c]	2.082[d]	2.094[e]	2.080[f]	
		2.209[c]		2.123[e]	2.070[f]	
		2.206[c]		2.107[e]	2.058[f]	
	(2.20)	(2.23)	(2.18)	(2.145)	(2.09)	
Bromide complexes						
Type	[h]	*cis*	*trans*	*trans*	[j]	*trans*
Br^-		2.629[i]	2.6682[f]	2.619[f]		3.082[f]
[1.96]		2.652[i]				2.426[f]
		(2.79)	(2.74)	(2.705)		(2.69)
$O(H_2)$		2.218[i]	2.112[f]	2.061[f]		1.93[f]
[1.40]		2.176[i]	2.077[f]	2.068[f]		
		2.216[i]				
		2.191[i]				
		(2.23)	(2.18)	(2.145)		(2.13)

[a] The numbers in [ ] and ( ) are the ionic radius and the sum of them, respectively. Data from ref. 27. [b] Data from ref. 11. [c] Data from ref. 13b. [d] Data from ref. 12b. [e] Data from ref. 7b. [f] This work. [g] Benrath [28] reported that no crystal of $CuCl_2 \cdot 4H_2O$ precipitates from $CuCl_2$ aqueous solution. [h] Crystal of $CrBr_2 \cdot 4H_2O$ has not been reported. [i] Data from ref. 14b. [j] It has not been reported that crystals of $NiBr_2 \cdot 4H_2O$ precipitate from $NiBr_2$ aqueous solutions [29, 30].

$2.70(3) \times 10^2$ pm and $O'(1) \cdots O'_{I}(2) = 2.69(2) \times 10^2$ pm.

The configurations and the metal–halide and metal–OH_2 bond lengths in the transition metal dihalide tetrahydrates determined in this study are summarized in comparison with those of the other complexes reported hitherto in Table 4. The sum of the ionic radii [27] are also included in Table 4, although the definition of the ionic radii of Cr^{2+} and Cu^{2+} is rather ambiguous, because they are actually not spherical. The structures around the metal ions in $CrCl_2 \cdot 4H_2O$, $FeCl_2 \cdot 4H_2O$, $FeBr_2 \cdot 4H_2O$ and $CoBr_2 \cdot 4H_2O$ have the *trans* configuration with respect to the halide ions, whereas those in $MnCl_2 \cdot 4H_2O$, $MnBr_2 \cdot 4H_2O$, $CoCl_2 \cdot 4H_2O$ and $NiCl_2 \cdot 4H_2O$ have the *cis* configuration. Interestingly, the structures of all the complexes with the *trans* configuration are axially elongated octahedral, while complexes with the *cis* configuration have all axially compressed structure.

From Table 4, the *cis*/*trans* stereoselectivity seems to depend on the transition metals except for the case of Co^{2+} dihalide complexes, in which $CoCl_2 \cdot 4H_2O$ has the *cis* configuration, while $CoBr_2 \cdot 4H_2O$ has the *trans* configuration, although the structures of some complexes are still unknown. The variation cannot be explained by a simple steric effect between the halide ions. The origin of the stereoselectivity is not yet clear. Several characteristics, however, are apparent from Table 4.

Among the complexes, those of $Cr^{2+}(d^4)$ and $Cu^{2+}(d^9)$ can be expected to have a strong Jahn–Teller effect. The length of the Cr–Cl bond in $CrCl_2 \cdot 4H_2O$ and the $Cu \cdots Br_I$ distance in $CuBr_2 \cdot 4H_2O$ are longer than those of the sum of the ionic radii, whereas all the other bond lengths are shorter than those expected from their ionic radii. The *trans* configuration constructing an axially elongated octahedron might be due to the Jahn–Teller effect. If $CrBr_2 \cdot 4H_2O$ and $CuCl_2 \cdot 4H_2O$ were crystallized, their crystal structures might be similar to those of $CrCl_2 \cdot 4H_2O$ [11] and $CuBr_2 \cdot 4H_2O$, respectively, due to the Jahn–Teller effect. The geometrical distortion of a number of transition metal ions has often been recognized to be closely related to the electronic structure in the d-orbitals. The *cis*/*trans* stereoselectivity found in the transition metal complexes may be strongly influenced by the electronic structure, including the Jahn–Teller effect.

The $CoCl_2 \cdot 4H_2O$ crystal has a *cis* form and $CoBr_2 \cdot 4H_2O$ a *trans* form. The difference may be explained in terms of the steric repulsion between Br^- ions which may be more significant than that between Cl^- ions because the former has a larger ionic size than the latter. This consideration includes the assumption that the Co^{2+} ion prefers a *cis*-configuration provided that the steric repulsive interaction between the halide ions is not significant. The ionic radius of Ni^{2+} is smaller than that of Co^{2+}, and thus the steric repulsion between Br^- ions is expected to be stronger than that of the Co^{2+} complex. If $NiBr_2 \cdot 4H_2O$ crystals were formed, the configuration around Ni^{2+} might be the *trans* form.

In addition, the effect arising from the hydrogen bonding should be taken into account as one of the factors which may affect the atomic packing in the crystal. Actually all these factors may contribute to the determination of the *cis*/*trans* configuration. The selectivity for the *cis*/*trans* configuration in the transition metal dihalide tetrahydrates is being studied by using *ab initio* MO calculations in order to discuss these effects more quantitatively.

Supplementary material

Tables of calculated and observed structure factors and lists of anisotropic thermal parameters are available on request.

Acknowledgement

The present work has been financially supported by a Grant-in-Aid for Scientific Research on Priority Area of "Molecular Approaches to Non-equilibrium Processes in Solution" (No. 02245106) from the Ministry of Education, Science and Culture, Japan.

References

1 B. Morosin and E. J. Graeber, *J. Chem. Phys.*, *42* (1965) 898.

2 B. Morosin, *J. Chem. Phys.*, *47* (1967) 417.

3 B. Morosin and E. J. Graeber, *Acta Crystallogr.*, *16* (1963) 1176.

4 B. Morosin, *Acta Crystallogr.*, *23* (1967) 630.

5 Å. Engberg, *Acta Chem. Scand.*, *24* (1970) 3510.

6 L. E. Orgel and J. D. Dunitz, *Nature (London)*, *179* (1957) 462.

7 (a) J. Mizuno, *J. Phys. Soc. Jpn.*, *15* (1960) 1412; (b) K. Waizumi, H. Masuda, H. Ohtaki, K. Tsukamoto and I. Sunagawa, *Bull. Chem. Soc. Jpn.*, *63* (1990) 3426.

8 (a) J. P. A. M. Hijmans, Q. A. G. van Vlimmeren and W. J. M. de Jonge, *Phys. Rev. B*, *12* (1975) 3859; (b) J. A. J. Basten and A. L. M. Bongaarts, *Phys. Rev. B*, *14* (1976) 2119; (c) K. Waizumi, H. Masuda and H. Ohtaki, unpublished work.

9 J. Mizuno, *J. Phys. Soc. Jpn.*, *16* (1961) 1574.

10 S. N. Bhatia, R. L. Carlin and A. P. Filho, *Physica B+C*, *92* (3) (1977) 330.

11 H. G. Von Schnering and B.-H. Brand, *Z. Anorg. Allg. Chem.*, *402* (1973) 159.

12 (a) B. R. Penfold and J. A. Grigor, *Acta Crystallogr.*, *12* (1959) 850; (b) P. J. Meunier-Piret and M. Van Meerssche, *Acta Crystallogr., Sect. B*, *27* (1971) 2329; (c) J. J. Verbist, W. C. Hamilton, T. F. Koetzle and M. S. Lehmann, *J. Chem. Phys.*, *56* (1972) 3257.

13 (a) A. Zalkin, J. D. Forrester and D. H. Templeton, *Inorg. Chem.*, *3* (1964) 529; (b) Z. M. El Saffar and G. M. Brown, *Acta Crystallogr., Sect. B*, *27* (1971) 66.

14 (a) K. Sudarsanan, *Acta Crystallogr., Sect. B*, *31* (1975) 2720; (b) E. D. Crozier and N. Alberding, *Acta Crystallogr., Sect. C*, *39* (1983) 808.

15 E. V. Stroganov, I. I. Kozina, S. N. Andreev and A. B. Koljadin, *Vestn. Leningr. Univ., Fiz. Khim.*, *15* (1960) 130.

16 J. N. McElearney, D. B. Losee, S. Merchant and R. L. Carlin, *Phys. Rev. B*, *7* (1973) 3314.

17 F. Schimmel, *Berichte*, *62B* (1929) 963.

18 A. Benrath and B. Schiffers, *Z. Anorg. Allg. Chem., 240* (1938) 67.

19 E. Boye, *Z. Anorg. Allg. Chem., 216* (1934) 29.

20 S. R. Carter and N. J. L. Megson, *J. Chem. Soc., 131* (1928) 2954.

21 N. Walker and D. Stuart, *Acta Crystallogr., Sect. A, 39* (1983) 158.

22 D. T. Cromer and J. T. Waber, *International Tables for X-ray Crystallography,* Vol. IV, Kynoch, Birmingham, UK, 1974, Table 2.2B.

23 D. T. Cromer, *International Tables for X-ray Crystallography,* Vol. IV, Kynoch, Birmingham, UK, 1974, Table 2.3.1.

24 B. A. Frenz, *Enraf-Nonius Structure Determination Package, SDP Users Guide,* Version 4, Enraf-Nonius, Delft, Netherlands, 1985.

25 T. Sakurai and K. Kobayashi, *Rikagaku Kenkyusho Houkoku, 55* (1979) 69.

26 C. K. Johnson, *ORTEP, Rep. ORNL-3794,* Oak Ridge National Laboratory, Oak Ridge, TN, 1965.

27 R. D. Shannon, *Acta Crystallogr., Sect. A, 32* (1976) 751.

28 H. Benrath, *Z. Anorg. Allg. Chem., 216* (1933) 207.

29 A. Etard, *Ann. Chim. Phys., 2* (7) (1894) 540.

30 I. Bolschakoff, *J. Russ. Phys. Chem. Soc., 29* (1897) 288.